1521-0103/365/2/272–280$35.00
THE JOURNAL OF PHARMACOLOGY AND EXPERIMENTAL THERAPEUTICS

https://doi.org/10.1124/jpet.117.247288
J Pharmacol Exp Ther 365:272–280, May 2018

Antiretroviral Drug Metabolism in Humanized PXR-CAR-CYP3A-NOG Mice[S]

JoEllyn M. McMillan, Denise A. Cobb, Zhiyi Lin, Mary G. Banoub, Raghubendra S. Dagur, Amanda A. Branch Woods, Weimin Wang, Edward Makarov, Ted Kocher, Poonam S. Joshi, Rolen M. Quadros, Donald W. Harms, Samuel M. Cohen, Howard E. Gendelman, Channabasavaiah B. Gurumurthy, Santhi Gorantla, and Larisa Y. Poluektova

Department of Pharmacology and Experimental Neuroscience (J.M.M., D.A.C., M.G.B., R.S.D., A.A.B.W., W.W., E.M., T.K., P.S. J., H.E.G., S.G., L.Y.P.), Developmental Neuroscience, Munroe Meyer Institute for Genetics and Rehabilitation (C.B.G.), Department of Pharmaceutical Sciences (Z.L.), Mouse Genome Engineering Core Facility, Vice Chancellor for Research Office (R.M.Q., D.W.H., C.B.G.), and Department of Pathology and Microbiology (S.M.C.), University of Nebraska Medical Center, Omaha, Nebraska

Received December 18, 2017; accepted February 22, 2018

ABSTRACT

Antiretroviral drug (ARV) metabolism is linked largely to hepatic cytochrome P450 activity. One ARV drug class known to be metabolized by intestinal and hepatic CYP3A are the protease inhibitors (PIs). Plasma drug concentrations are boosted by CYP3A inhibitors such as cobisistat and ritonavir (RTV). Studies of such drug-drug interactions are limited since the enzyme pathways are human specific. While immune-deficient mice reconstituted with human cells are an excellent model to study ARVs during human immunodeficiency virus type 1 (HIV-1) infection, they cannot reflect human drug metabolism. Thus, we created a mouse strain with the human pregnane X receptor, constitutive androstane receptor, and CYP3A4/7 genes on a NOD.Cg-*Prkdc*^{scid} *Il2rg*^{tm1Sug}/JicTac background (hCYP3A-NOG) and used them to evaluate the impact of human CYP3A metabolism on ARV pharmacokinetics. In proof-of-concept studies we used nanoformulated atazanavir (nanoATV) with or without RTV. NOG and hCYP3A-NOG mice were treated weekly with 50 mg/kg nanoATV alone or boosted with nanoformulated ritonavir (nanoATV/r). Plasma was collected weekly and liver was collected at 28 days post-treatment. Plasma and liver atazanavir (ATV) concentrations in nanoATV/r-treated hCYP3A-NOG mice were 2- to 4-fold higher than in replicate NOG mice. RTV enhanced plasma and liver ATV concentrations 3-fold in hCYP3A-NOG mice and 1.7-fold in NOG mice. The results indicate that human CYP3A-mediated drug metabolism is reduced compared with mouse and that RTV differentially affects human gene activity. These differences can affect responses to PIs in humanized mouse models of HIV-1 infection. Importantly, hCYP3A-NOG mice reconstituted with human immune cells can be used for bench-to-bedside translation.

Introduction

Humanized immunodeficient mice are now considered a suitable model for studies of human immunodeficiency virus (HIV) type 1 (HIV-1) disease pathobiology and therapy (McCune et al., 1990; Merry et al., 1997; André et al., 1998; Riska et al., 1999; Limoges et al., 2001; Stoddart et al., 2007; Denton et al., 2008; Donia et al., 2010; Sango et al., 2010; Dash et al., 2012; Nischang et al., 2012; Roy et al., 2012; Speck, 2015). To serve such goals CIEA NOG (Ito et al., 2002) or NOD.Cg-*Prkdc*^{scid} *Il2rg*^{tm1Wjl}/SzJ mice (NOD scid gamma mice; The Jackson Laboratory; Bar Harbor, ME) are reconstituted with human CD34$^+$ hematopoietic stem cells (Ishikawa et al., 2005; Gorantla et al., 2012; Gonzalez et al., 2013; Marsden and Zack, 2017). Work in our own laboratory and those of others have shown the application of this animal model for testing long-acting antiretroviral (ARV) drug nanoformulations developed for both pre-exposure prophylaxis and treatment of existing infections (Dash et al., 2012; Puligujja et al., 2015a; Kirtane et al., 2016; Zhang et al., 2016; Edagwa et al., 2017; Zhou et al., 2018). Prior studies on nanoformulated ritonavir-boosted atazanavir (nanoATV/r) administered weekly demonstrated sustained plasma drug concentrations and suppressed HIV-1 infection with concomitant restoration in CD4$^+$ T-cell numbers (Dash et al., 2012). Although humanized mice serve as valuable tools to assess antiretroviral efficacy, divergences in drug metabolism between humans and rodents makes translation of studies from rodents to humans difficult.

This work was supported by a University of Nebraska Medical Center Graduate Student Fellowship and the National Institutes of Health [Grants R24OD018546, P01DA028555, R01NS036126, and R01AG043540].
https://doi.org/10.1124/jpet.117.247288.
[S] This article has supplemental material available at jpet.aspetjournals.org.

ABBREVIATIONS: ARV, antiretroviral; ATV, atazanavir; AUC, area under the concentration-time curve; CAR, constitutive androstane receptor; HIV, human immunodeficiency virus; HIV-1, human immunodeficiency virus type 1; LC, liquid chromatography; MS, mass spectrometry; nanoATV, nanoformulated atazanavir; nanoATV/r, nanoformulated ritonavir-boosted atazanavir; nanoRTV, nanoformulated ritonavir; P450, cytochrome P450; PCR, polymerase chain reaction; PI, protease inhibitor; PXR, pregnane X receptor; RTV, ritonavir; UPLC, ultra-performance liquid chromatography.

Most ARV interactions occur through inhibition or induction of hepatic drug metabolism. These are linked, in the largest measure, to the cytochrome P450 (P450) monooxygenase system. The enzymes are transcriptionally regulated by ligand-activated transcription factors such as the aryl hydrocarbon receptor, pregnane X receptor (PXR), and constitutive androstane receptor (CAR) (Handschin and Meyer, 2003). Similar to the P450 enzymes, PXR and CAR can bind multiple different ligands and their ligand specificity varies across species (Timsit and Negishi, 2007). Overlapping ligand specificity between PXR and CAR, species specificity in ligand binding, and the opposing effects of these receptors' activities make the net effect of xenobiotic regulation of major P450s complex (Moore et al., 2000). For HIV-1 pharmacology there are challenges associated with multiple drug combinations. Thus there is a need to characterize, understand, and limit drug-drug interactions in the context of human drug metabolism.

As a clinically relevant example, for the HIV-1 protease inhibitors (PIs) lopinavir, atazanavir (ATV), and darunavir, intestinal absorption and hepatic elimination are largely governed by CYP3A4/5 activity (Shen et al., 1997). PI pharmacokinetic profiles are boosted by ritonavir (RTV) or cobicistat primarily through their inhibition of CYP3A enzymatic activity (Hull and Montaner, 2011). When used in HIV-1 treatment regimens, PIs with low-dose RTV (300/100 mg) are administered in combination with nucleoside reverse transcriptase inhibitors such as abacavir, lamivudine, tenofovir, and/or emtricitabine (van Heeswijk et al., 2001). Ritonavir-boosted atazanavir (ATV/r) may also be used alone as maintenance therapy (Achenbach et al., 2011; Tsai et al., 2017).

While drug boosting is an important aspect of HIV-1 therapeutic regimens, the means to study such drug-drug interactions are limited since the enzyme pathways and regulation are commonly human specific (Martignoni et al., 2006; Gautam et al., 2014). Human and mouse PXR and CAR show significant homology in *CYP3A* binding sites; however, homology in their ligand-binding domains is limited (Xie et al., 2000; Owen and Curley, 2015; Yan and Xie, 2016). Consequently, there are significant species differences in ligand activation of PXR and CAR and induction of CYP3A (Xie et al., 2000; Gibson et al., 2002).

We sought to modify the humanized mouse model in ways that would permit examination of human liver drug metabolizing enzymes and regulatory proteins, broadening its utility beyond studies of virus-cell-tissue interactions and ARV pharmacokinetics. To these ends, we generated a transgenic mouse with targeted replacement of mouse to human PXR, CAR, and CYP3A4/7 genes (Taconic model 11585, or PXR-CAR-CYP3A4/3A7, abbreviated hCYP3A) on a CIEA NOG mouse background. The created mice were used to evaluate the impact of human CYP3A metabolism on the pharmacokinetics of nanoformulated ATV/r (nanoATV/r) treatment (Roy et al., 2012). Plasma and liver ATV concentrations following treatment with nanoATV/r were 2- to 4-fold greater than in control mice. Cotreatment with nanoATV/r provided an approximate 3-fold enhancement of plasma and liver ATV concentrations over nanoformulated ATV (nanoATV) alone. Clear sex-dependent differences were observed for the plasma area under the concentration-time curve (AUC) and liver ATV concentrations in the nanoATV/r-treated transgenic mice. The plasma ATV AUC was 1.3-fold higher in female mice and liver ATV concentration was 1.9-fold higher in males. Taken together, a mouse model that contains the human PXR, CAR, and CYP3A4/7 genes on a genetic background suitable for humanization could be employed for studies of drug-drug interactions (Merry et al., 1997; Riska et al., 1999; van Waterschoot et al., 2010; Dellamonica et al., 2012; Holmstock et al., 2013; Scheer and Roland Wolf, 2013). These mice show clear applications for drug development and translation.

Materials and Methods

Materials. Optima and liquid chromatography (LC)/mass spectrometry (MS) grade solvents were obtained from Fisher Scientific (Waltham, MA). Poloxamer 407 was purchased from Sigma-Aldrich (St. Louis, MO). ATV-sulfate, purchased from Gyma Laboratories of America Inc. (Westbury, MA) was free-based using triethylamine. Free-based RTV was purchased from Shengda Pharmaceutical Co. (Zhejiang, China).

Generation and Characterization of hCYP3A-NOG Mice. Humanized PXR-CAR-CYP3A4/3A7 (hCYP3A) (C57BL/6-*Nr1i3*$^{tm1(NR1I3)Arte}$Is(5CYP3A4-CYP3A7;Del5Cyp3a57-Cyp3a59)2Arte*Nr1i2*$^{tm1(NR1I2)Arte}$) and NOG mice were obtained from Taconic Biosciences (Hudson, NY). Mice were kept in microisolator cages with free access to food and water. Light cycles were 12:12 hour light/dark with the light phasing starting at 6:00 AM. Temperature and humidity were maintained between 21°C and 23°C and 45% and 65%, respectively. The hCYP3A strain was backcrossed to the NOG strain through a marker-assisted speed congenics protocol established in our laboratory (Gurumurthy et al., 2015). Genotypes of the mice were identified using standard polymerase chain reaction (PCR)–based genotyping reactions as previously described (Harms et al., 2014; Quadros et al., 2016). Briefly, either tail or ear piece DNA was collected from each individual animal and put into a tube containing 300 μl cell lysis buffer and 20 μl proteinase K (20 mg/ml). The mixture was kept overnight in a dry bath set at 65°C. DNA was extracted using the Qiagen Gentra Puregene Tissue Kit (Qiagen Sciences, Germantown, MD) and stored at 4°C for future use. For PCR reaction, 2× GoTaq Green Master Mix (Promega Life Sciences, Madison, WI) was diluted to 1× with nuclease free water, and 1 μl forward primer and 1 μl reverse primer (100 μM stocks) per sample were added for 100 μl master mix to a 2 ml microcentrifuge tube; 15 μl of master mix per sample and 1 μl of genomic DNA was added to the PCR tubes. The samples were then placed in a Bio-Rad T100 Thermal Cycler (Bio-Rad Laboratories, Hercules, CA) for amplification. Amplified products were run on a 1.5% agarose gel and analyzed via a Kodak Gel Logic 212 Imaging system (Eastman Kodak Co., Rochester, NY). Five separate PCR reactions are required to properly genotype humanized PXR-CAR-CYP3A4/3A7 mice (Supplemental Fig. 1).

A duplex PCR reaction, containing three primers, could be used for identifying both the mutant and wild-type alleles for CAR mutation, whereas two separate PCRs were needed to identify mutant and wild-type alleles for the PXR and CYP34A4 alleles. At the end of the speed congenics breeding, the heterozygous offspring were intercrossed to obtain homozygous mutations for all three loci. The primer sets used for genotyping are listed in Supplemental Table 1.

Ritonavir-Boosted Atazanavir Nanoformulations. Poloxamer 407-coated nanoATV and nanoformulated RTV (nanoRTV) were prepared by high-pressure homogenization and characterized for size, size distribution, and zeta potential as previously described (Balkundi et al., 2011; Puligujja et al., 2013). The nanosuspensions were lyophilized and drug loading was determined by reversed-phase high-performance LC (Nowacek et al., 2009). The lyophilized drug nanosuspensions were resuspended in phosphate-buffered saline and injected intramuscularly in a total injection volume of 40 μl per 25 g mouse. Injection solutions were prepared fresh, just prior to use on treatment days. To ensure adequate homogeneous suspension, the suspensions were sonicated for 10 seconds prior to injection and

vortexed frequently during treatment of animals. Drug content in the injection solutions was determine by ultra-performance LC (UPLC) tandem MS as described previously (Huang et al., 2011).

Pharmacokinetics and Drug Metabolism. Animal studies were performed in accordance with the Guidelines for the Care and Use of Laboratory Animals mandated by the U.S. National Institutes of Health (Bethesda, MD; https://www.ncbi.nlm.nih.gov/books/NBK54050/) and the University of Nebraska Medical Center Institutional Animal Care and Use Committee. Male and female mice, 3 to 4 months of age, were used.

The newly developed transgenic mice (hCYP3A-NOG) and wild-type (NOG) mice were treated intramuscularly with nanoATV alone (50 mg/kg) or a combination of nanoATV and nanoRTV (nanoATV/r) (20 or 50 mg/kg each drug) on days 0, 3, 7, 14, and 21. The numbers of male and female mice ($N \geq 3$) in each treatment group were the same for each strain (hCYP3A-NOG and NOG). Serial blood samples were collected on days 1, 3, 7, 14, 21, and 28 into heparinized tubes and plasma prepared. Tissues were collected on day 28 (Fig. 1).

Plasma and Tissue Collection. Fifty microliters of whole blood was collected into heparinized tubes by submandibular puncture on days 1, 3, 7, 14, and 21 (prior to injection of next dose) and 1 ml by cardiac puncture on the day of sacrifice. The blood samples were centrifuged at 3000*g* and plasma was collected. The plasma samples were stored at −80°C until analysis. Tissues were collected at the time of animal sacrifice. Half of each tissue was flash frozen in liquid nitrogen and stored at −80°C for drug quantitation and gene expression. The other half was fixed in 10% neutral buffered formalin for histopathology.

Quantitation of ATV and RTV. ATV and RTV concentrations in plasma and liver were determined by UPLC tandem MS as previously described with minor modifications (Huang et al., 2011). Briefly, 100 mg liver was homogenized in four volumes of LC/MS-grade water. One milliliter of ice-cold Optima-grade acetonitrile was added to 25 μl of plasma or 100 μl liver homogenate prespiked with 10 μl internal standard (2.0 μg/ml lopinavir, 200 ng/ml final concentration). Samples were vortexed continuously for 3 minutes and centrifuged at 16,000*g* for 10 minutes at 4°C. The supernatants were collected and evaporated under vacuum at room temperature and then reconstituted in 100 μl of 50% Optima-grade methanol in water and sonicated for 5 minutes. After centrifugation (16,000*g*; 10 minutes; 4°C), 10 μl of each sample was analyzed by UPLC tandem MS for drug quantitation using a Waters Acquity H-class UPLC coupled to a Waters Xevo TQ-S Micro Triple Quadrupole Mass Spectrometer (Waters, Milford, MA). Chromatographic separation was achieved on a Waters Acquity BEH Shield RP 18 column (1.7 μm, 100 × 2.1 mm) affixed with an Acquity UPLC C18 guard column. The mobile phase consisted of (A) 5% Optima-grade acetonitrile in methanol and (B) 7.5 mM ammonium acetate adjusted to pH 4.0 with glacial acetic acid at a flow rate of 0.28 ml/min. Samples were eluted using a gradient of 70% A for 5.0 minutes, increased to 90% A over 1.0 minutes, held at 90% A for 0.8 minutes, reset to 70% A over 1.0 minutes, and then held for 1.0 minutes for column re-equilibration. ATV and RTV were quantitated using drug-to-internal-standard peak area ratios and drug calibration curves of 0.2–2000 ng/ml. ATV, RTV, and lopinavir were detected using multiple reactions monitoring transitions of 705.24 > 168.065, 721.14 > 296.104, and 629.177 > 447.202, respectively.

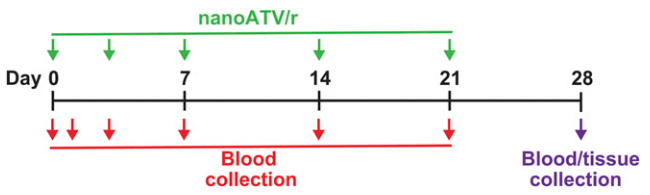

Fig. 1. Experimental timeline for nanoformulated drug treatment and blood and tissue collection. NanoATV/r or nanoATV were administered on days 0, 3, 7, 14, and 21 by intramuscular injection to hCYP3A-NOG and NOG mice. Whole blood was collected into heparinized tubes on days 1, 3, 7, 14, 21, and 28 and plasma was prepared. Liver tissue was collected at day 28.

Gene Expression Analyses. For relative gene expression, livers from hCYP3A-NOG and NOG mice were homogenized and total RNA was extracted using RNeasy Plus Universal Kit (Qiagen Sciences) following the manufacturer's instructions. An equal amount of RNA (1 μg) was used to reverse transcribe into cDNA using a cDNA synthesis kit (ThermoFisher Scientific, Waltham, MA) in 40 μl reaction volume. Real-time PCR was performed on a StepOne Plus PCR (Applied Biosystems, Foster City, CA) in a singleplex 20 μl mix with human-specific (PXR, Hs00243666_m1; CAR, Hs00231959_m1; and CYP3A4, Hs00604506_m1) and mouse-specific (mPXR, Mm00803092_m1; Cyp3a11, Mm00731567_m1; mCAR, Mm01170117_m1 and Actb, Mm00607939_s1) primer-probe sets and Taqman gene expression master mix (Applied Biosystems) using 1 μl cDNA. Real-time PCR settings were as follows: 50°C for 2 minutes, and then 95°C for 10 minutes, followed by 40 cycles of 95°C for 15 seconds and 60°C for 1 minute (Dagur et al., 2018). Fluorescence intensity was measured at each change of temperature to monitor amplification. Target gene expression was determined using the comparative threshold cycle method and normalized to an endogenous mouse β-actin. Fold increase in gene expression was calculated as a ratio of normalized expression in drug-treated to untreated animals.

Histopathology. At the study end, liver tissue samples were fixed with 10% neutral buffered formalin and embedded in paraffin. Five-micron-thick sections were stained with hematoxylin and eosin. Histopathology was evaluated according to the guidelines of the Society of Toxicologic Pathology (Reston, VA; https://focusontoxpath.com/hepatotoxicity/).

Statistical Analyses. The plasma AUC and statistical differences were determined using GraphPad Prism 7.0 (GraphPad Software Inc., LaJolla, CA). Statistical differences between the AUCs for different groups were determined using Student's *t* test. Statistical differences between tissue drug concentrations were determined using one-way analysis of variance with Tukey's multiple comparisons tests. Differences in male and female tissue drug concentrations were determined using two-way ANOVA with uncorrected Fisher's LSD. Differences in mRNA induction of CYP3A, PXR, and CAR genes were determined by one-tailed Student's *t* test. The criterion for statistical significance was $P < 0.05$.

Results

Generation and Characterization of the hCYP3A-NOG Mice. Homozygous hCYP3A-NOG transgenic mice were viable and fertile with no differences from the parent NOG strain. However, hCYP3A-NOG males and females showed lower body weight compared with NOG mice (Supplemental Fig. 2). Drug treatment induced a mild reduction of parent NOG mice body weight by the end of the observation (Supplemental Figs. 2 and 3). The effect was most pronounced in NOG males treated with 50 mg/kg nanoATV/r. Importantly, no drug-related histopathological changes were observed in the livers of the mice (Supplemental Fig. 4) following nanoATV/r treatment.

RTV Affects ATV Plasma and Liver Concentrations in hCYP3A-NOG Mice. RTV is used to boost plasma ATV concentrations in patients through inhibition of CYP3A activity (Cooper et al., 2003; Arya et al., 2012). Previous studies in our laboratory have demonstrated that weekly administration of nanoATV/r to wild-type mice (Balb/cJ, C57Bl/6, NOD scid gamma mice) provided sustained plasma ATV concentrations (Dash et al., 2012; Gautam et al., 2013, 2014). However, neither mice nor nonhuman primates completely reflected drug boosting (Martignoni et al., 2006; Gautam et al., 2014).

To determine the effect of an RTV boost, hCYP3A-NOG and NOG mice were treated weekly with nanoATV/r and plasma drug concentrations were monitored over 28 days. As shown in Fig. 2A, ATV plasma concentrations were 2- to 5-fold higher in hCYP3A-NOG mice compared with NOG mice in all treatment groups. The difference (4- to 5-fold) was most pronounced at the higher dose (50 mg/kg) at days 7–28. The AUC for plasma ATV in animals treated with 50 mg/kg nanoATV/r was 4.2-fold higher in hCYP3A-NOG mice compared with NOG mice (Table 1). In contrast, RTV plasma concentrations and AUCs were similar in both mouse strains (Fig. 2B; Table 1). RTV boosted ATV concentrations to a greater extent in hCYP3A-NOG mice than NOG mice. RTV boosted plasma ATV concentrations at day 28 by 3-fold in hCYP3A-NOG mice compared with 2-fold in NOG mice. The AUC for 50 mg/kg nanoATV/r was 2.7-fold greater than the AUC for 50 mg/kg nanoATV (19430 vs. 7111) in the transgenic mice, whereas the difference in wild-type mice was 1.9-fold (4590 vs. 2402) (Table 1). Interestingly, the ATV plasma concentrations on days 1–21 were 1.4- to 1.8-fold higher in hCYP3A-NOG females given 50 mg/kg nanoATV/r compared with males given the same treatment (Fig. 3A), which translated into an increased AUC ($P = 0.04$) in females (Table 1). This sex difference was not observed in NOG mice. No sex differences were observed in either strain for plasma RTV concentrations (Fig. 3B; Table 1).

The differences in plasma ATV concentrations between the mouse strains reflected differences in liver ATV concentrations. As shown in Fig. 4A, liver ATV concentrations were higher in hCYP3A-NOG mice compared with NOG mice following treatment with either 20 mg/kg (1.9-fold, 667.1 vs. 338.4 ng/g) or 50 mg/kg (3.2-fold, 3225 vs. 1002 ng/g) nanoATV/r. Inclusion of RTV boosted ATV liver concentrations by 3.2-fold ($P < 0.05$) in hCYP3A-NOG mice but not NOG mice. RTV liver concentrations were significantly higher (2-fold) in hCYP3A-NOG mice compared with NOG mice treated with 50 mg/kg nanoATV/r (Fig. 4B).

Liver ATV concentrations were significantly higher (1.9-fold) in hCYP3A-NOG males compared with females treated with 50 mg/kg nanoATV/r (4065 vs. 2105 ng/g; $P < 0.001$) (Fig. 5A). No significant sex differences were observed in mice treated with 20 mg/kg nanoATV/r or nanoATV alone. In contrast, no sex differences in liver ATV concentrations were observed in NOG mice treated with either 20 or 50 mg/kg nanoATV/r. Liver RTV concentrations were also significantly higher in hCYP3A-NOG males compared with females treated with 50 mg/kg nanoATV/r, while no differences were observed in RTV liver concentrations between NOG males and females (Fig. 5B).

Expression of CYP3A, PXR, and CAR in Livers of hCYP3A-NOG and NOG Mice. Differences in expression of human and mouse CYP3A, PXR, and CAR genes were determined in livers of mice treated with nanoATV alone or nanoATV/r. Induction (fold increase over control) of mRNA expression for human (hCYP3A-NOG) and mouse (NOG) CYP3A4/7, PXR, and CAR was determined by real-time PCR. Induction of CYP3A4, PXR, and CAR by nanoATV and nanoATV/r was greater in both male and female hCYP3A-NOG mice compared with NOG mice (Fig. 6). CYP3A4 induction was 0.5- to 14-fold in NOG females compared with 80- to 113-fold in replicate hCYP3A-NOG mice. Responses differed in male mice compared with female mice. Induction of CYP3A4 and PXR was moderately higher in hCYP3A-NOG mice compared with NOG mice with nanoATV/r treatment. However, in contrast to the response in females, CAR induction was much greater in NOG males compared with hCYP3A-NOG males. The expression of CYP3A7, known to be expressed in human fetal liver but not adult liver (Lacroix et al., 1997; Pang et al., 2012; Betts et al., 2015), was very low in our adult mouse livers and was not induced by drug treatments (data not shown).

Discussion

Our laboratories have developed a new NOG strain of mouse containing the human PXR, CAR, and CYP3A4/7 genes. These mice, with similar survival rates and fertility to wild-type NOG mice (data not shown), were used to assess the pharmacokinetics of weekly administered nanoATV/r. There were significant differences in ATV plasma and liver concentrations and induction of CYP3A4, PXR, and CAR between the two strains. Importantly, the observed differences in ATV plasma and liver concentrations were greater in humanized mice (2.7-fold) compared with wild-type mice (1.9-fold). Cotreatment with nanoRTV boosted plasma ATV concentrations in both male and female mice (Fig. 2). These results were similar to our previous studies wherein weekly subcutaneous or intramuscular administration of nanoATV and nanoRTV

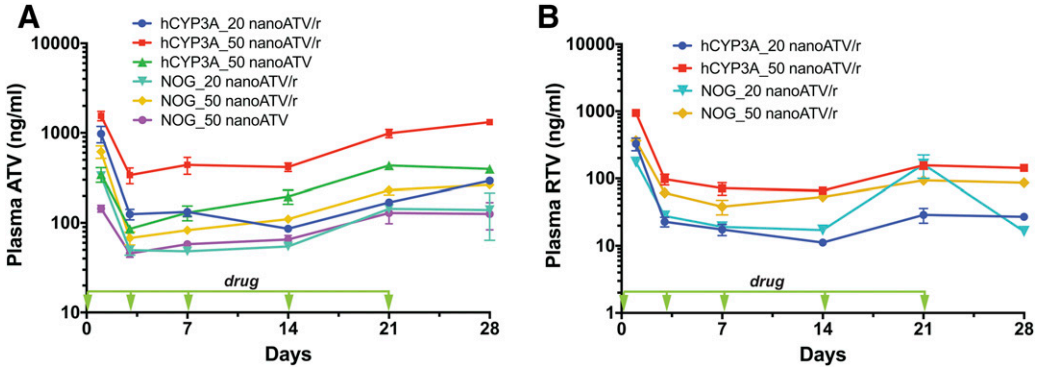

Fig. 2. Drug plasma concentrations in nanoATV or nanoATV/r-treated mice. (A) ATV plasma concentrations in humanized hCYP3A-NOG (hCYP3A) or NOG mice treated intramuscularly with 20 or 50 mg/kg nanoATV/r or 50 mg/kg nanoATV on days 0, 3, 7, 14, and 21. (B) RTV plasma concentrations in hCYP3A and NOG mice treated with 20 or 50 mg/kg nanoATV/r. Data are expressed as mean ± S.E.M. $N = 5–8$.

TABLE 1

AUC for plasma ATV and RTV

Data are expressed as average (ng d/ml) ± S.E.M. Significantly different from NOG mice value: *$P < 0.05$; ****$P < 0.0001$. Significantly different from 50 mg/kg nanoATV/r treated mice of similar strain: †$P < 0.05$; ††$P < 0.001$.

Strain and Treatment	N	ATV	RTV
		ng d/ml	*ng d/ml*
hCYP3A-NOG mice, 20 mg/kg nanoATV/r			
All	8	4891 ± 663*	868 ± 229
Male	5	4498 ± 686	663 ± 77
Female	3	5548 ± 730	1209 ± 306
hCYP3A-NOG mice, 50 mg/kg nanoATV/r			
All	7	19,430 ± 2058****	3687 ± 439
Male	4	16,729 ± 1309	3023 ± 463
Female	3	23,031 ± 2110[a]	4457 ± 584
hCYP3A-NOG mice, 50 mg/kg nanoATV			
All	5	7111 ± 717††	
NOG mice, 20 mg/kg nanoATV/r			
All	8	2621 ± 781	1674 ± 863
Male	5	2201 ± 234	1778 ± 1088
Female	3	3322 ± 1237	1498 ± 453
NOG mice, 50 mg/kg nanoATV/r			
All	7	4590 ± 516	2087 ± 217
Male	4	4101 ± 198	2056 ± 339
Female	3	5242 ± 654	2130 ± 300
NOG mice, 50 mg/kg nanoATV			
All	5	2402 ± 486†	

[a]Significantly different from nanoATV/r male mice of similar strain and treatment ($P < 0.05$).

provided sustained plasma ATV levels in Balb/cJ mice (Dash et al., 2012; Roy et al., 2012; Gautam et al., 2014; Puligujja et al., 2015a,b), which were boosted by cotreatment with nanoRTV. Furthermore, preliminary studies using the Taconic model 11585 (PXR-CAR-CYP3A4/3A7) C57Bl/6 background mice treated with weekly doses of nanoATV/r showed 5-fold higher ATV plasma concentrations at study end compared with wild-type mice (unpublished data). The RTV boost observed in the new strain of mice was equivalent to that observed in wild-type C57Bl/6 mice (Gautam et al., 2014). Importantly, no evidence of necrosis or acute inflammation was observed in either hCYP3A-NOG or NOG mice in the current study, which mirrored our previous observations (Dash et al., 2012; Gautam et al., 2014).

Differences in male and female responses to ARVs are well known in humans (Ofotokun, 2005) and may be associated with sex-related differences in regulation of drug metabolizing enzymes and transporters (Ofotokun, 2005). In the present study, sex differences in ATV and RTV plasma concentrations were observed in hCYP3A-NOG mice, with higher plasma ATV concentrations in females compared to males given 50 mg/kg nanoATV/r. In addition, the RTV boosting effects were 2-fold greater in female humanized mice (2.7-fold) compared with female wild-type mice (1.3-fold). Higher plasma ATV concentrations in female hCYP3A-NOG mice reflect sex differences in ATV concentrations reported in humans during treatment (Ofotokun and Pomeroy, 2003). These differences in turn may be related to a lower risk of viral control failure in women compared with men, but a higher rate of treatment discontinuation (Svedhem-Johansson et al., 2013). Our data may also predict ARV toxicity profiling, as demonstrated by the association of ATV plasma concentrations exceeding that required for viral control (upper therapeutic threshold) with a higher risk of liver and kidney dysfunction (Gervasoni et al., 2015).

The predictive value of mice with human drug metabolizing enzymes and regulatory proteins for drug-drug interaction studies have been demonstrated by a variety of other studies.

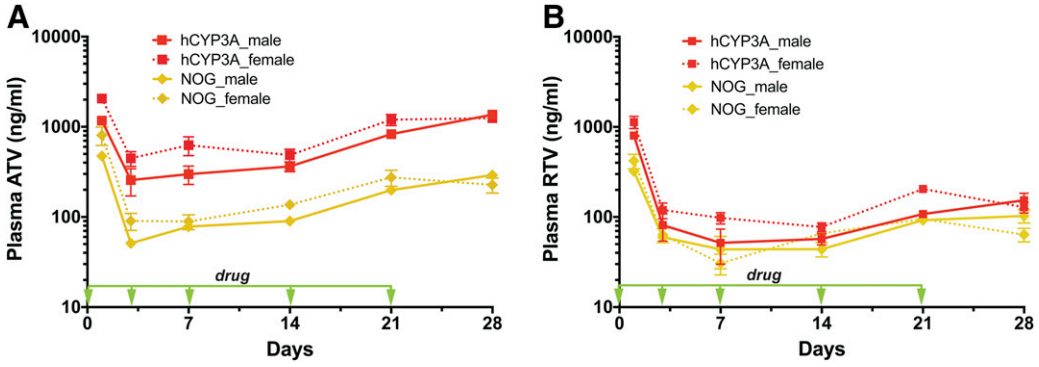

Fig. 3. Sex-dependent differences in plasma drug concentrations in mice treated with nanoATV/r. ATV (A) and RTV (B) plasma concentrations over time in humanized hCYP3A-NOG (hCYP3A) and NOG male and female mice treated intramuscularly with 50 mg/kg nanoATV/r on days 0, 3, 7, 14, and 21. Data are expressed as mean ± S.E.M. $N = 3$ (female) or 4 (male).

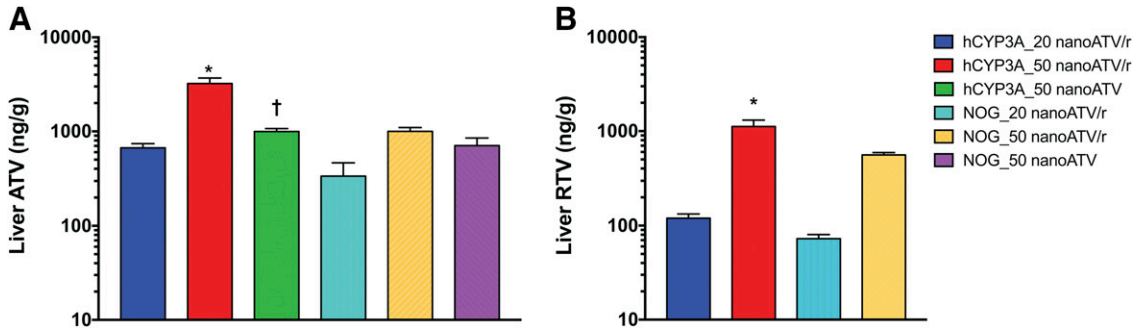

Fig. 4. Liver drug concentrations in hCYP3A-NOG (hCYP3A) and NOG mice. Mice were treated intramuscularly with 20 or 50 mg/kg nanoATV/r or 50 mg/kg nanoATV on days 0, 3, 7, 14, and 21 and livers were collected on day 28. Liver ATV (A) and RTV (B) concentrations were determined by UPLC tandem MS. Data are expressed as mean ± S.E.M. *Significantly different than similarly treated NOG mice ($P < 0.05$). †Significantly different than hCYP3A mice treated with 50 mg/kg nanoATV/r ($P < 0.05$).

The relative induction of rifampicin, sulfinpyrazone, and pioglitazone on CYP3A4 expression and pharmacokinetics of triazolam in hu-PXR-CAR-CYP3A4/7 mice was shown to be reflective of the human responses (Hasegawa et al., 2011). In another study, CYP3A-humanized mice were used to demonstrate RTV boosting of a new protease inhibitor NVS123 (Das et al., 2016). These humanized mice can also provide predictive information of the generation of human-specific drug metabolites as was shown by Nishimura et al. (2013) for clemizole in TK-NOG mice transplanted with human hepatocytes. Humanization of not only hepatic but also intestinal CYP3A is important for predicting human drug metabolites as demonstrated in studies by Nakada et al. (2016). The metabolite profile of the antidepressant drug nefazodone in murine CYP3A knockout mice with humanized livers (*Cyp3a* knockout chimeric mice) mirrored that observed in humans. Similarly, Barzi et al. (2017) observed human-type metabolism of ATV in PIRF mice repopulated with human hepatocytes when the murine NADPH-P450 oxidoreductase gene was deleted. The importance of CYP3A in generation of toxic ATV and RTV metabolites was shown by Li et al. (2011a,b). In immune competent C57Bl/6 background hu-PXR-CAR-CYP3A4/7 mice, differences in the metabolite profile of drugs in combination compared with normal mice have been shown for itraconazole/cobimetinib and midazolam plus the CYP3A inhibitor clarithromycin and support our observations for the interactions of ATV and RTV (Choo et al., 2015; Ly et al., 2017).

For adequate suppression of HIV replication and to reduce the development of viral drug resistance, plasma PI concentrations need to be maintained at therapeutic levels. Thus, clinically, RTV has been used to boost plasma PI concentrations (Hsu et al., 1998; Condra et al., 2000) through inhibition of CYP3A4 metabolism of PIs by intestinal epithelial cells and hepatocytes and through inhibition of the P-glycoprotein efflux transporter in intestinal epithelial cells (Holmstock et al., 2012). However, the action of RTV in humans is not straightforward. RTV inhibits CYP3A liver and intestinal activity by 70%, but can also induce CYP3A4 activity through activation of PXR (Luo et al., 2002). Using our new hCYP3A-NOG strain of mice we observed the net outcome for injectable long-acting formulations that exhibit complex interactions resulting from induction and inhibition of P450 enzymes.

The critical role of PXR and CAR in the regulation of phase I (oxidation) and phase II (conjugation) drug metabolizing enzymes and transporters, their selectivity for different ligands including endogenous lipids and hormones, their influence on inflammatory responses (Kusunoki et al., 2014), and their regulation of cholesterol, glucose, and lipid metabolism (Li et al., 2007; Timsit and Negishi, 2007; Moreau et al., 2008; Yan et al., 2015) can elicit distinct differences between mice and humans. For example, the synthetic glucocorticoid dexamethasone is a more potent inducer of Cyp3a in wild-type mice compared with mice humanized for PXR (Scheer et al., 2010). In another study, PXR and CAR humanized mice, but not wild-type mice, displayed increased microsomal protein

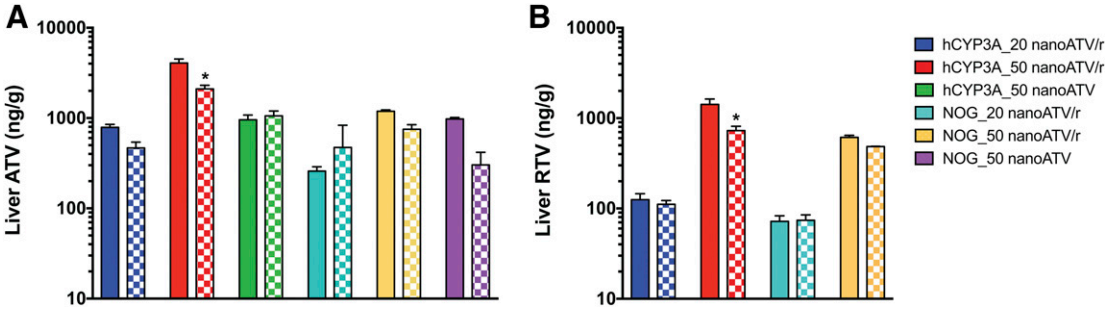

Fig. 5. Sex-dependent differences in liver drug concentrations in mice treated with nanoATV/r. Mice were treated intramuscularly with 20 or 50 mg/kg nanoATV/r or 50 mg/kg nanoATV on days 0, 3, 7, 14, and 21 and livers were collected on day 28. Liver ATV (A) and RTV (B) concentrations were determined by UPLC tandem MS. Males, solid bars; females, hatched bars. Data are expressed as mean ± S.E.M. *Significantly different than respectively treated male mice ($P < 0.05$). $N = 4$ to 5 (nanoATV/r-treated males); $N = 3$ (nanoATV/r-treated females; nanoATV-treated males); $N = 2$ (nanoATV-treated females).

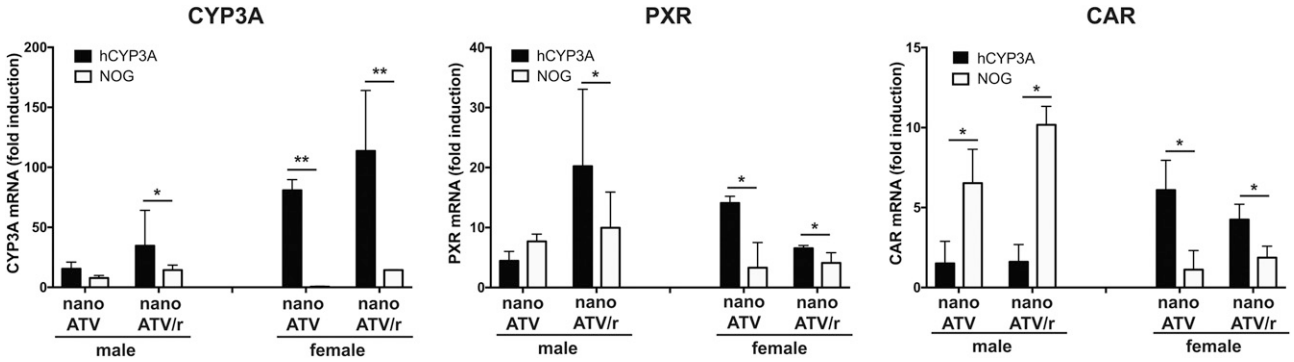

Fig. 6. Liver CYP3A4, PXR, and CAR mRNA levels in mice treated with nanoATV or nanoATV/r. Expression of human and mouse genes for CYP3A4, PXR, and CAR in liver were determined by real-time PCR using human (hCYP3A) and mouse (NOG) specific primers in mice treated with 50 mg/kg nanoATV or 50 mg/kg nanoATV/r. Significant differences were determined by one-tailed Students *t* test at $^{*}P < 0.05$; $^{**}P < 0.01$. $N = 4$ to 5 (nanoATV/r-treated males); $N = 3$ (nanoATV/r-treated females; nanoATV-treated males); $N = 2$ (nanoATV-treated females).

content, total P450 content, and P450 reductase activity in response to rifampicin treatment (Lee et al., 2009). Species-specific differences in PXR and CAR activation and their regulation of energy metabolism may also underlie the differences in body weight in the hCYP3A-NOG and control NOG mice and the slight weight loss following treatment in NOG mice observed in the current study. Differences in such responses and substrate specificities can markedly influence the translation of studies for drug bioavailability, distribution, toxicity, and efficacy from mice to humans. The new humanized immune-deficient mouse strain offers the potential for studying human PXR and CAR regulation of drug metabolism and inflammatory responses in the context of drug treatment of immune-mediated disease.

Limitations of this humanized mouse model are that it does not emulate human variability of gene expressions, does not incorporate polymorphisms in drug metabolizing enzymes that influence therapeutic efficacy and toxicity, and does not incorporate humanization of drug efflux transporters such as P-glycoprotein that affect PI distribution in sanctuary sites (e.g., brain, vaginal mucosa, testes) (Griffin et al., 2011). The non-nucleoside reverse transcriptase inhibitor efavirenz can activate PXR and promote CYP3A4 activity in patients on ARV treatment (Hariparsad et al., 2004; Fellay et al., 2005), and a single nucleotide polymorphism in PXR is associated with ATV plasma trough levels below the minimum effective concentration (Siccardi et al., 2008). Furthermore, while these mice are useful in examining the human/mouse differences in PXR and CAR regulation and CYP3A4 metabolism of ARVs, other drug metabolizing enzymes and transporters also contribute to the bioavailability and pharmacokinetics of ARVs. As an example, ATV is a substrate for CYP3A5, P-glycoprotein, multidrug resistance protein 1, and human organic anion transporters, and an inhibitor of P-glycoprotein and breast cancer resistance protein (Bousquet et al., 2008; Janneh et al., 2009; Achenbach et al., 2011). CYP2D6, with well-known poor and extensive metabolizer polymorphism, can contribute variably to the metabolism of RTV (Kumar et al., 1996; Hsu et al., 1998; Kaspera et al., 2014). In addition, RTV induces CYP2B6, which contributes to the metabolism of PIs as well as efavirenz (Dixit et al., 2007; Foisy et al., 2008). Thus, species differences and polymorphisms in substrate specificities and activities in these enzymes and transporters could affect the pharmacokinetics and drug-drug interactions observed for ARVs in this humanized mouse model.

In addition, the downstream genetic and protein responses are those of the mouse, not humans. Despite these limitations, the hu-PXR-CAR-CYP3A4/7 model can provide predictive values for the development of drug combinations with reduced drug-drug interactions and toxicities. The important advantage of the new hCYP3A-NOG mouse strain is their suitability for immune reconstitution by transplantation of human hematopoietic stem cells and human tissue tumor xenografts that will provide human-like metabolism of combinations of ARV and anticancer drugs. This new strain of mice could also be used for testing drug combinations related to treatment of cancers not previously associated with HIV, such as lung, head and neck, liver, anal, and kidney cancers, which occur in HIV-infected individuals at much higher rates than in the general population (Deeken et al., 2015).

For future studies, this new strain of immune deficient mice will be used to determine the biologic activities of clinically used ARV combinations and for development of long-acting formulations of these ARVs in human $CD34^{+}$ hematopoietic stem cell-reconstituted HIV-1 infected animals.

Acknowledgments

We acknowledge the technical assistance of Diana Palandri and Celina Prince.

Authorship Contributions

Participated in research design: Poluektova, McMillan, Gendelman, Gorantla, Gurumurthy.

Conducted experiments: Cobb, Lin, Banoub, Dagur, Makarov.

Contributed new reagents or analytic tools: Branch Woods, Wang, Joshi, Quadros, Harms, Gurumurthy.

Performed data analysis: Poluektova, McMillan, Dagur, Kocher, Cohen.

Wrote or contributed to the writing of the manuscript: McMillan, Poluektova, Gendelman, Gurumurthy.

References

Achenbach CJ, Darin KM, Murphy RL, and Katlama C (2011) Atazanavir/ritonavir-based combination antiretroviral therapy for treatment of HIV-1 infection in adults. *Future Virol* **6**:157–177.

André P, Groettrup M, Klenerman P, de Giuli R, Booth BL, Jr, Cerundolo V, Bonneville M, Jotereau F, Zinkernagel RM, and Lotteau V (1998) An inhibitor of HIV-1 protease modulates proteasome activity, antigen presentation, and T cell responses. *Proc Natl Acad Sci USA* **95**:13120–13124.

Arya V, Robertson SM, Struble KA, and Murray JS (2012) Scientific considerations for pharmacoenhancers in antiretroviral therapy. *J Clin Pharmacol* **52**:1128–1133.

Balkundi S, Nowacek AS, Veerubhotla RS, Chen H, Martinez-Skinner A, Roy U, Mosley RL, Kanmogne G, Liu X, Kabanov AV, et al. (2011) Comparative manufacture and cell-based delivery of antiretroviral nanoformulations. *Int J Nanomedicine* **6**:3393–3404.

Barzi M, Pankowicz FP, Zorman B, Liu X, Legras X, Yang D, Borowiak M, Bissig-Choisat B, Sumazin P, Li F, et al. (2017) A novel humanized mouse lacking murine P450 oxidoreductase for studying human drug metabolism. *Nat Commun* **8**:39.
Betts S, Björkhem-Bergman L, Rane A, and Ekström L (2015) Expression of CYP3A4 and CYP3A7 in human foetal tissues and its correlation with nuclear receptors. *Basic Clin Pharmacol Toxicol* **117**:261–266.
Bousquet L, Roucairol C, Hembury A, Nevers MC, Creminon C, Farinotti R, and Mabondzo A (2008) Comparison of ABC transporter modulation by atazanavir in lymphocytes and human brain endothelial cells: ABC transporters are involved in the atazanavir-limited passage across an in vitro human model of the blood-brain barrier. *AIDS Res Hum Retroviruses* **24**:1147–1154.
Choo EF, Woolsey S, DeMent K, Ly J, Messick K, Qin A, and Takahashi R (2015) Use of transgenic mouse models to understand the oral disposition and drug-drug interaction potential of cobimetinib, a MEK inhibitor. *Drug Metab Dispos* **43**: 864–869.
Condra JH, Petropoulos CJ, Ziermann R, Schleif WA, Shivaprakash M, and Emini EA (2000) Drug resistance and predicted virologic responses to human immunodeficiency virus type 1 protease inhibitor therapy. *J Infect Dis* **182**:758–765.
Cooper CL, van Heeswijk RP, Gallicano K, and Cameron DW (2003) A review of low-dose ritonavir in protease inhibitor combination therapy. *Clin Infect Dis* **36**:1585–1592.
Dagur RS, Wang W, Cheng Y, Makarov E, Ganesan M, Suemizu H, Gebhart CL, Gorantla S, Osna N, and Poluektova LY (2018) Human hepatocyte depletion in the presence of HIV-1 infection in dual reconstituted humanized mice. *Biol Open* **7**:2. pii: bio029785.
Das R, Strowig T, Verma R, Koduru S, Hafemann A, Hopf S, Kocoglu MH, Borsotti C, Zhang L, Branagan A, et al. (2016) Microenvironment-dependent growth of preneoplastic and malignant plasma cells in humanized mice. *Nat Med* **22**:1351–1357.
Dash PK, Gendelman HE, Roy U, Balkundi S, Alnouti Y, Mosley RL, Gelbard HA, McMillan J, Gorantla S, and Poluektova LY (2012) Long-acting nanoformulated antiretroviral therapy elicits potent antiretroviral and neuroprotective responses in HIV-1-infected humanized mice. *AIDS* **26**:2135–2144.
Deeken JF, Beumer JH, Anders NM, Wanjiku T, Rusnak M, and Rudek MA (2015) Preclinical assessment of the interactions between the antiretroviral drugs, ritonavir and efavirenz, and the tyrosine kinase inhibitor erlotinib. *Cancer Chemother Pharmacol* **76**:813–819.
Dellamonica P, Di Perri G, and Garraffo R (2012) NNRTIs: pharmacological data. *Med Mal Infect* **42**:287–295.
Denton PW, Estes JD, Sun Z, Othieno FA, Wei BL, Wege AK, Powell DA, Payne D, Haase AT, and Garcia JV (2008) Antiretroviral pre-exposure prophylaxis prevents vaginal transmission of HIV-1 in humanized BLT mice. *PLoS Med* **5**:e16.
Dixit V, Hariparsad N, Li F, Desai P, Thummel KE, and Unadkat JD (2007) Cytochrome P450 enzymes and transporters induced by anti-human immunodeficiency virus protease inhibitors in human hepatocytes: implications for predicting clinical drug interactions. *Drug Metab Dispos* **35**:1853–1859.
Donia M, McCubrey JA, Bendtzen K, and Nicoletti F (2010) Potential use of rapamycin in HIV infection. *Br J Clin Pharmacol* **70**:784–793.
Edagwa B, McMillan J, Sillman B, and Gendelman HE (2017) Long-acting slow effective release antiretroviral therapy. *Expert Opin Drug Deliv* **14**:1281–1291.
Fellay J, Marzolini C, Decosterd L, Golay KP, Baumann P, Buclin T, Telenti A, and Eap CB (2005) Variations of CYP3A activity induced by antiretroviral treatment in HIV-1 infected patients. *Eur J Clin Pharmacol* **60**:865–873.
Foisy MM, Yakiwchuk EM, and Hughes CA (2008) Induction effects of ritonavir: implications for drug interactions. *Ann Pharmacother* **42**:1048–1059.
Gautam N, Puligujja P, Balkundi S, Thakare R, Liu XM, Fox HS, McMillan J, Gendelman HE, and Alnouti Y (2014) Pharmacokinetics, biodistribution, and toxicity of folic acid-coated antiretroviral nanoformulations. *Antimicrob Agents Chemother* **58**:7510–7519.
Gautam N, Roy U, Balkundi S, Puligujja P, Guo D, Smith N, Liu XM, Lamberty B, Morsey B, Fox HS, et al. (2013) Preclinical pharmacokinetics and tissue distribution of long-acting nanoformulated antiretroviral therapy. *Antimicrob Agents Chemother* **57**:3110–3120.
Gervasoni C, Meraviglia P, Minisci D, Ferraris L, Riva A, Landonio S, Cozzi V, Charbe N, Molinari L, Rizzardini G, et al. (2015) Metabolic and kidney disorders correlate with high atazanavir concentrations in HIV-infected patients: is it time to revise atazanavir dosages? *PLoS One* **10**:e0123670.
Gibson GG, Plant NJ, Swales KE, Ayrton A, and El-Sankary W (2002) Receptor-dependent transcriptional activation of cytochrome P4503A genes: induction mechanisms, species differences and interindividual variation in man. *Xenobiotica* **32**:165–206.
Gonzalez L, Strbo N, and Podack ER (2013) Humanized mice: novel model for studying mechanisms of human immune-based therapies. *Immunol Res* **57**: 326–334.
Gorantla S, Gendelman HE, and Poluektova LY (2012) Can humanized mice reflect the complex pathobiology of HIV-associated neurocognitive disorders? *J Neuroimmune Pharmacol* **7**:352–362.
Griffin L, Annaert P, and Brouwer KL (2011) Influence of drug transport proteins on the pharmacokinetics and drug interactions of HIV protease inhibitors. *J Pharm Sci* **100**:3636–3654.
Gurumurthy CB, Joshi PS, Kurz SG, Ohtsuka M, Quadros RM, Harms DW, and Lloyd KC (2015) Validation of simple sequence length polymorphism regions of commonly used mouse strains for marker assisted speed congenics screening. *Int J Genomics* **2015**:735845.
Handschin C and Meyer UA (2003) Induction of drug metabolism: the role of nuclear receptors. *Pharmacol Rev* **55**:649–673.
Hariparsad N, Nallani SC, Sane RS, Buckley DJ, Buckley AR, and Desai PB (2004) Induction of CYP3A4 by efavirenz in primary human hepatocytes: comparison with rifampin and phenobarbital. *J Clin Pharmacol* **44**:1273–1281.
Harms DW, Quadros RM, Seruggia D, Ohtsuka M, Takahashi G, Montoliu L, and Gurumurthy CB (2014) Mouse genome editing using the CRISPR/Cas system. *Curr Protoc Hum Genet* **83**:15.7.1–15.7.27.
Hasegawa M, Kapelyukh Y, Tahara H, Seibler J, Rode A, Krueger S, Lee DN, Wolf CR, and Scheer N (2011) Quantitative prediction of human pregnane X receptor and cytochrome P450 3A4 mediated drug-drug interaction in a novel multiple humanized mouse line. *Mol Pharmacol* **80**:518–528.
Holmstock N, Annaert P, and Augustijns P (2012) Boosting of HIV protease inhibitors by ritonavir in the intestine: the relative role of cytochrome P450 and P-glycoprotein inhibition based on Caco-2 monolayers versus in situ intestinal perfusion in mice. *Drug Metab Dispos* **40**:1473–1477.
Holmstock N, Gonzalez FJ, Baes M, Annaert P, and Augustijns P (2013) PXR/CYP3A4-humanized mice for studying drug-drug interactions involving intestinal P-glycoprotein. *Mol Pharm* **10**:1056–1062.
Hsu A, Granneman GR, and Bertz RJ (1998) Ritonavir. Clinical pharmacokinetics and interactions with other anti-HIV agents. *Clin Pharmacokinet* **35**:275–291.
Huang J, Gautam N, Bathena SP, Roy U, McMillan J, Gendelman HE, and Alnouti Y (2011) UPLC-MS/MS quantification of nanoformulated ritonavir, indinavir, atazanavir, and efavirenz in mouse serum and tissues. *J Chromatogr B Analyt Technol Biomed Life Sci* **879**:2332–2338.
Hull MW and Montaner JS (2011) Ritonavir-boosted protease inhibitors in HIV therapy. *Ann Med* **43**:375–388.
Ishikawa F, Yasukawa M, Lyons B, Yoshida S, Miyamoto T, Yoshimoto G, Watanabe T, Akashi K, Shultz LD, and Harada M (2005) Development of functional human blood and immune systems in NOD/SCID/IL2 receptor gamma chain(null) mice. *Blood* **106**:1565–1573.
Ito M, Hiramatsu H, Kobayashi K, Suzue K, Kawahata M, Hioki K, Ueyama Y, Koyanagi Y, Sugamura K, Tsuji K, et al. (2002) NOD/SCID/γ_c^{null} mouse: an excellent recipient mouse model for engraftment of human cells. *Blood* **100**:3175–3182.
Janneh O, Anwar T, Jungbauer C, Kopp S, Khoo SH, Back DJ, and Chiba P (2009) P-glycoprotein, multidrug resistance-associated proteins and human organic anion transporting polypeptide influence the intracellular accumulation of atazanavir. *Antivir Ther* **14**:965–974.
Kaspera R, Kirby BJ, Sahele T, Collier AC, Kharasch ED, Unadkat JD, and Totah RA (2014) Investigating the contribution of CYP2J2 to ritonavir metabolism in vitro and in vivo. *Biochem Pharmacol* **91**:109–118.
Kirtane AR, Langer R, and Traverso G (2016) Past, present, and future drug delivery systems for antiretrovirals. *J Pharm Sci* **105**:3471–3482.
Kumar GN, Rodrigues AD, Buko AM, and Denissen JF (1996) Cytochrome P450-mediated metabolism of the HIV-1 protease inhibitor ritonavir (ABT-538) in human liver microsomes. *J Pharmacol Exp Ther* **277**:423–431.
Kusunoki Y, Ikarashi N, Hayakawa Y, Ishii M, Kon R, Ochiai W, Machida Y, and Sugiyama K (2014) Hepatic early inflammation induces downregulation of hepatic cytochrome P450 expression and metabolic activity in the dextran sulfate sodium-induced murine colitis. *Eur J Pharm Sci* **54**:17–27.
Lacroix D, Sonnier M, Moncion A, Cheron G, and Cresteil T (1997) Expression of CYP3A in the human liver—evidence that the shift between CYP3A7 and CYP3A4 occurs immediately after birth. *Eur J Biochem* **247**:625–634.
Lee HM, Wu W, Wysoczynski M, Liu R, Zuba-Surma EK, Kucia M, Ratajczak J, and Ratajczak MZ (2009) Impaired mobilization of hematopoietic stem/progenitor cells in C5-deficient mice supports the pivotal involvement of innate immunity in this process and reveals novel promobilization effects of granulocytes. *Leukemia* **23**:2052–2062.
Li F, Lu J, and Ma X (2011a) Metabolomic screening and identification of the bioactivation pathways of ritonavir. *Chem Res Toxicol* **24**:2109–2114.
Li F, Lu J, Wang L, and Ma X (2011b) CYP3A-mediated generation of aldehyde and hydrazine in atazanavir metabolism. *Drug Metab Dispos* **39**:394–401.
Li T, Chen W, and Chiang JY (2007) PXR induces CYP27A1 and regulates cholesterol metabolism in the intestine. *J Lipid Res* **48**:373–384.
Limoges J, Poluektova L, Ratanasuwan W, Rasmussen J, Zelivyanskaya M, McClernon DR, Lanier ER, Gendelman HE, and Persidsky Y (2001) The efficacy of potent anti-retroviral drug combinations tested in a murine model of HIV-1 encephalitis. *Virology* **281**:21–34.
Luo G, Cunningham M, Kim S, Burn T, Lin J, Sinz M, Hamilton G, Rizzo C, Jolley S, Gilbert D, et al. (2002) CYP3A4 induction by drugs: correlation between a pregnane X receptor reporter gene assay and CYP3A4 expression in human hepatocytes. *Drug Metab Dispos* **30**:795–804.
Ly JQ, Messick K, Qin A, Takahashi RH, and Choo EF (2017) Utility of CYP3A4 and PXR-CAR-CYP3A4/3A7 transgenic mouse models to assess the magnitude of CYP3A4 mediated drug-drug interactions. *Mol Pharm* **14**:1754–1759.
Marsden MD and Zack JA (2017) Humanized mouse models for human immunodeficiency virus infection. *Annu Rev Virol* **4**:393–412.
Martignoni M, Groothuis GM, and de Kanter R (2006) Species differences between mouse, rat, dog, monkey and human CYP-mediated drug metabolism, inhibition and induction. *Expert Opin Drug Metab Toxicol* **2**:875–894.
McCune JM, Namikawa R, Shih CC, Rabin L, and Kaneshima H (1990) Suppression of HIV infection in AZT-treated SCID-hu mice. *Science* **247**:564–566.
Merry C, Barry MG, Mulcahy F, Ryan M, Heavey J, Tjia JF, Gibbons SE, Breckenridge AM, and Back DJ (1997) Saquinavir pharmacokinetics alone and in combination with ritonavir in HIV-infected patients. *AIDS* **11**:F29–F33.
Moore LB, Parks DJ, Jones SA, Bledsoe RK, Consler TG, Stimmel JB, Goodwin B, Liddle C, Blanchard SG, Willson TM, et al. (2000) Orphan nuclear receptors constitutive androstane receptor and pregnane X receptor share xenobiotic and steroid ligands. *J Biol Chem* **275**:15122–15127.
Moreau A, Vilarem MJ, Maurel P, and Pascussi JM (2008) Xenoreceptors CAR and PXR activation and consequences on lipid metabolism, glucose homeostasis, and inflammatory response. *Mol Pharm* **5**:35–41.
Nakada N, Kawamura A, Kamimura H, Sato K, Kazuki Y, Kakuni M, Ohbuchi M, Kato K, Tateno C, Oshimura M, et al. (2016) Murine *Cyp3a* knockout chimeric mice with humanized liver: prediction of the metabolic profile of nefazodone in humans. *Biopharm Drug Dispos* **37**:3–14.
Nischang M, Sutmuller R, Gers-Huber G, Audigé A, Li D, Rochat MA, Baenziger S, Hofer U, Schlaepfer E, Regenass S, et al. (2012) Humanized mice recapitulate key

features of HIV-1 infection: a novel concept using long-acting anti-retroviral drugs for treating HIV-1. *PLoS One* **7**:e38853.
Nishimura T, Hu Y, Wu M, Pham E, Suemizu H, Elazar M, Liu M, Idilman R, Yurdaydin C, Angus P, et al. (2013) Using chimeric mice with humanized livers to predict human drug metabolism and a drug-drug interaction [published correction appears in *J Pharmacol Exp Ther.* (2013) 345:327]. *J Pharmacol Exp Ther* **344**:388–396.
Nowacek AS, Miller RL, McMillan J, Kanmogne G, Kanmogne M, Mosley RL, Ma Z, Graham S, Chaubal M, Werling J, et al. (2009) NanoART synthesis, characterization, uptake, release and toxicology for human monocyte-macrophage drug delivery. *Nanomedicine (Lond)* **4**:903–917.
Ofotokun I (2005) Sex differences in the pharmacologic effects of antiretroviral drugs: potential roles of drug transporters and phase 1 and 2 metabolizing enzymes. *Top HIV Med* **13**:79–83.
Ofotokun I and Pomeroy C (2003) Sex differences in adverse reactions to antiretroviral drugs. *Top HIV Med* **11**:55–59.
Owen A and Curley P (2015) Species similarities and differences in pharmacokinetics and distribution of antiretroviral drugs, in *Humanized Mice for HIV Research* (Poluektova L, Garcia J, Koyanagi Y, Manz M, and Tager A eds) pp 339–360, Springer, New York.
Pang XY, Cheng J, Kim JH, Matsubara T, Krausz KW, and Gonzalez FJ (2012) Expression and regulation of human fetal-specific CYP3A7 in mice. *Endocrinology* **153**:1453–1463.
Puligujja P, Araínga M, Dash P, Palandri D, Mosley RL, Gorantla S, Poluektova L, McMillan J, and Gendelman HE (2015a) Pharmacodynamics of folic acid receptor targeted antiretroviral nanotherapy in HIV-1-infected humanized mice. *Antiviral Res* **120**:85–88.
Puligujja P, Balkundi SS, Kendrick LM, Baldridge HM, Hilaire JR, Bade AN, Dash PK, Zhang G, Poluektova LY, Gorantla S, et al. (2015b) Pharmacodynamics of long-acting folic acid-receptor targeted ritonavir-boosted atazanavir nanoformulations. *Biomaterials* **41**:141–150.
Puligujja P, McMillan J, Kendrick L, Li T, Balkundi S, Smith N, Veerubhotla RS, Edagwa BJ, Kabanov AV, Bronich T, et al. (2013) Macrophage folate receptor-targeted antiretroviral therapy facilitates drug entry, retention, antiretroviral activities and biodistribution for reduction of human immunodeficiency virus infections. *Nanomedicine (Lond)* **9**:1263–1273.
Quadros RM, Poluektova LY, and Gurumurthy CB (2016) Simple and reliable genotyping protocol for mouse *Prkdc*^{SCID} mutation. *J Immunol Methods* **431**:60–62.
Riska PS, Joseph DP, Dinallo RM, Davidson WC, Keirns JJ, and Hattox SE (1999) Biotransformation of nevirapine, a non-nucleoside HIV-1 reverse transcriptase inhibitor, in mice, rats, rabbits, dogs, monkeys, and chimpanzees. *Drug Metab Dispos* **27**:1434–1447.
Roy U, McMillan J, Alnouti Y, Gautum N, Smith N, Balkundi S, Dash P, Gorantla S, Martinez-Skinner A, Meza J, et al. (2012) Pharmacodynamic and antiretroviral activities of combination nanoformulated antiretrovirals in HIV-1-infected human peripheral blood lymphocyte-reconstituted mice. *J Infect Dis* **206**:1577–1588.
Sango K, Joseph A, Patel M, Osiecki K, Dutta M, and Goldstein H (2010) Highly active antiretroviral therapy potently suppresses HIV infection in humanized Rag2$^{-/-}\gamma_c^{-/-}$ mice. *AIDS Res Hum Retroviruses* **26**:735–746.
Scheer N and Roland Wolf C (2013) Xenobiotic receptor humanized mice and their utility. *Drug Metab Rev* **45**:110–121.
Scheer N, Ross J, Kapelyukh Y, Rode A, and Wolf CR (2010) In vivo responses of the human and murine pregnane X receptor to dexamethasone in mice. *Drug Metab Dispos* **38**:1046–1053.
Shen DD, Kunze KL, and Thummel KE (1997) Enzyme-catalyzed processes of first-pass hepatic and intestinal drug extraction. *Adv Drug Deliv Rev* **27**:99–127.
Siccardi M, D'Avolio A, Baietto L, Gibbons S, Sciandra M, Colucci D, Bonora S, Khoo S, Back DJ, Di Perri G, et al. (2008) Association of a single-nucleotide polymorphism in the pregnane X receptor (*PXR* 63396C→T) with reduced concentrations of unboosted atazanavir. *Clin Infect Dis* **47**:1222–1225.
Speck RF (2015) Antiretroviral treatment testing in HIV-infected humanized mice, in *Humanized Mice for HIV Research* (Poluektova LY, Victor Garcia J, Koyanagi Y, Manz MG, and Tager AM eds) pp 361–380, Springer, New York.
Stoddart CA, Bales CA, Bare JC, Chkhenkeli G, Galkina SA, Kinkade AN, Moreno ME, Rivera JM, Ronquillo RE, Sloan B, et al. (2007) Validation of the SCID-hu Thy/Liv mouse model with four classes of licensed antiretrovirals. *PLoS One* **2**: e655.
Svedhem-Johansson V, Pugliese P, Brockmeyer NH, Thalme A, Michalik C, Esser S, Barlet MH, Nakonz T, and Jimenez-Exposito MJ (2013) Long-term gender-based outcomes for atazanavir/ritonavir (ATV/r)-containing regimens in treatment-experienced patients with HIV. *Curr HIV Res* **11**:333–341.
Timsit YE and Negishi M (2007) CAR and PXR: the xenobiotic-sensing receptors. *Steroids* **72**:231–246.
Tsai MS, Chang SY, Lin SW, Kuo CH, Sun HY, Wu BR, Tang SY, Liu WC, Su YC, Hung CC, et al. (2017) Treatment response to unboosted atazanavir in combination with tenofovir disoproxil fumarate and lamivudine in human immunodeficiency virus-1-infected patients who have achieved virological suppression: a therapeutic drug monitoring and pharmacogenetic study. *J Microbiol Immunol Infect* **50**: 789–797.
van Heeswijk RP, Veldkamp A, Mulder JW, Meenhorst PL, Lange JM, Beijnen JH, and Hoetelmans RM (2001) Combination of protease inhibitors for the treatment of HIV-1-infected patients: a review of pharmacokinetics and clinical experience. *Antivir Ther* **6**:201–229.
van Waterschoot RA, ter Heine R, Wagenaar E, van der Kruijssen CM, Rooswinkel RW, Huitema AD, Beijnen JH, and Schinkel AH (2010) Effects of cytochrome P450 3A (CYP3A) and the drug transporters P-glycoprotein (MDR1/ABCB1) and MRP2 (ABCC2) on the pharmacokinetics of lopinavir. *Br J Pharmacol* **160**: 1224–1233.
Xie W, Barwick JL, Downes M, Blumberg B, Simon CM, Nelson MC, Neuschwander-Tetri BA, Brunt EM, Guzelian PS, and Evans RM (2000) Humanized xenobiotic response in mice expressing nuclear receptor SXR. *Nature* **406**:435–439.
Yan J, Chen B, Lu J, and Xie W (2015) Deciphering the roles of the constitutive androstane receptor in energy metabolism. *Acta Pharmacol Sin* **36**:62–70.
Yan J and Xie W (2016) A brief history of the discovery of PXR and CAR as xenobiotic receptors. *Acta Pharm Sin B* **6**:450–452.
Zhang G, Guo D, Dash PK, Araínga M, Wiederin JL, Haverland NA, Knibbe-Hollinger J, Martinez-Skinner A, Ciborowski P, Goodfellow VS, et al. (2016) The mixed lineage kinase-3 inhibitor URMC-099 improves therapeutic outcomes for long-acting antiretroviral therapy. *Nanomedicine (Lond)* **12**:109–122.
Zhou T, Su H, Dash P, Lin Z, Dyavar Shetty BL, Kocher T, Szlachetka A, Lamberty B, Fox HS, Poluektova L, et al. (2018) Creation of a nanoformulated cabotegravir prodrug with improved antiretroviral profiles. *Biomaterials* **151**:53–65.

Address correspondence to: Dr. Larisa Y. Poluektova, Department of Pharmacology and Experimental Neuroscience, University of Nebraska Medical Center, Omaha, NE 68198. E-mail: lpoluekt@unmc.edu; or Dr. Channabasavaiah B. Gurumurthy, Developmental Neuroscience, Munroe Meyer Institute for Genetics and Rehabilitation, University of Nebraska Medical Center, Omaha, NE 68198. E-mail: cgurumurthy@unmc.edu; or Dr. JoEllyn M. McMillan, Department of Pharmacology and Experimental Neuroscience, University of Nebraska Medical Center, Omaha, NE 68198. E-mail: jmmcmillan@unmc.edu